Design and Assessment of Delay Timer Alarm Systems for Nonlinear Chemical Processes

Aditya Tulsyan[a,*], Feras Alrowaie[b], R. Bhushan Gopaluni[c]

[a] *Department of Chemical Engineering, Massachusetts Institute of Technology, Cambridge, Massachusetts, 02139, USA.*
[b] *Department of Chemical and Process Engineering Technology, Jubail Industrial College, Jubail Industrial City 31961, KSA.*
[c] *Department of Chemical and Biological Engineering, University of British Columbia, Vancouver, BC V6T 1Z3, Canada.*

Abstract

In process and manufacturing industries, alarm systems play a critical role in ensuring safe and efficient operations. The objective of a standard industrial alarm system is to detect undesirable deviations in process variables as soon as they occur. Fault detection and diagnosis (FDD) systems often need to be alerted by an industrial alarm system; however, poorly designed alarms often lead to alarm flooding and other undesirable events. In this paper, we consider the problem of industrial alarm design for processes represented by stochastic nonlinear time-series models. The alarm design for such complex processes faces three important challenges: 1) industrial processes exhibit highly nonlinear behavior; 2) state variables are not precisely known (modeling error); and 3) process signals are not necessarily Gaussian, stationary or uncorrelated. In this paper, a procedure for designing a delay timer alarm configuration is proposed for the process states. The proposed design is based on minimization of the rate of false and missed alarm rates – two common performance measures for alarm systems. To ensure the alarm design is robust to any non-stationary process behavior, an expected-case and a worst-case alarm designs are proposed. Finally, the efficacy of the proposed alarm design is illustrated on a non-stationary chemical reactor problem.

Keywords: Alarm design, nonlinear systems, alarm performance, SMC methods

[☆] This work was supported by the Shri Gopal Rajgarhia International Research Scholar Support Program, IIT Kharagpur, India. A shorter version of this work[1] was published in the 2016 American Control Conference.

[*] Corresponding author. *Tel:*+1 617 314 1608

Email addresses: tulsyan@mit.edu (Aditya Tulsyan), rowaie_fa@jic.edu.sa (Feras Alrowaie), bhushan.gopaluni@ubc.ca (R. Bhushan Gopaluni)

Introduction

Modern process industries are equipped with highly automated fault detection and diagnosis (FDD) systems to maintain process safety and reliability standards. The primary objective of an alarm system is to alert the plant operator every time a fault occurs or the process deviates from its normal behavior. According to the Abnormal Situation Management Consortium (ASM), the US petrochemical plants alone lose more than $10 billion per year due to abnormal plant situations and from the lack of an efficient alarm management strategies.[2] A recent global survey conducted in different countries around the world, including the USA, the UK, Canada, the Europe Union and Japan, indicated that about 42% of abnormal operations were caused due to human error alone as shown in Figure 3. This is partly due to the complex tasks performed by the plant operators that include presentation, processing, and handling of thousands of alarm signals generated by different unit operations in a process plant. As process and manufacturing industries pace toward increased automation by deploying a large number of smart sensors, without an efficient alarm management system in place, process monitoring is expected to become an increasingly daunting task.[3]

An efficient alarm system is critical for setting up an efficient FDD system; however, there is a subtle difference between the FDD algorithms[4,5] and the alarm design algorithms. The FDD algorithms are designed to work online to identify faults by appropriately processing the measurements while the process is running. On the other hand, alarms are designed offline prior to starting a process and the design is not changed online. FDD algorithms are often designed to identify specific known faults whereas alarms are designed for almost every measured process variable. In fact, all industrial sensor measurements are by default given appropriate alarm limits in the distributed control systems.

The design and performance evaluation of alarm systems has received considerable attention from the academic and industrial communities.[6,7,8] While an alarm installation and operations involve a number of key steps that include the design, processing, presentation and management, the alarm design has received little attention. The alarm design is a critical first step in setting up an efficient alarm management system. Many industrial incidents, for example, the *Deepwater Horizon oil spill* in 2010,[9] the *Buncefield fire* in 2005,[10] the *BP Texas City refinery explosion* in 2005[11] have been attributed in parts to the poor design of

alarm systems.

An alarm design method can be classified as either a signal-based or a model-based design method.[12] While, the model-based design methods rely on comparing the actual process behavior against the expected predicted normal behavior, the signal-based methods largely rely on the historical process data and *a priori* process knowledge.[13,14] The signal-based methods are generally the method of choice for alarm designs in process industries. This is because (i) the signal-based methods do not require any process models, which are nontrivial to build for industrial systems, and (b) the resulting alarm designs can be readily implemented on almost all modern distributed computer systems (DCS) and supervisor control and data acquisition (SCADA) systems. In contrast, the model-based design methods, although less commonly used in process industry, tend to be more accurate provided high-quality models are available.[6] In general, obtaining a high-accuracy model for complex industrial processes is nontrivial, barring for smaller unit operations, such as reactors and heat-exchangers, where high-accuracy models can still be developed in a reasonable amount of time.

For the model and data-based alarm design methods, the most common alarm generation procedure is the simple limit-checking method; wherein, an alarm is generated by comparing the signal with the alarm threshold.[6,13] See Figure 4(a) for illustration. The signal illustrated in Figure 4(a) is a generic signal, and can either represent the actual process variable being monitored, as often the case is in a signal-based method or alternatively, it can also represent a residual signal generated in a model-based method. In Figure 4(a), the simple limit-checking method generates an alarm every time the signal crosses the threshold.

Despite the simplicity of the limit-checking method, a proper selection of the alarm threshold is critical for it directly influences the rate (or probability) of false and missed alarms (FAR/MAR) – a common measure of alarm performance. A false alarm (false positive) is an alarm that is raised while the process is still in normal operations, and a missed alarm (false negative) occurs when the alarm is not raised even when the process is behaving abnormally (see Figure 4(b) for illustration). For instance, for the alarm threshold chosen in Figure 4(a), several samples in the normal operations (i.e., for time ≤ 125) fall above the alarm limit thereby causing false alarms. Similarly, several samples in the abnormal operations (i.e., for

time > 125) fall below the alarm limit thereby causing missed alarms. Figure 4(b) represents the state of the alarm for the signal in Figure 4(a). Technically, the false and missed alarms are both detrimental to the safe-process operation and should be minimized for an improved alarm performance.

To reduce the rates of false and missed alarms, and to desensitize the alarm systems to external process noise and disturbances, delay timers are commonly used.[15,16] A standard n-sample on-delay timer is an alarm configuration that is triggered when the process variable is continuously over the alarm threshold for at least n samples. Similarly, once the alarm is raised, it is cleared only if m consecutive samples go below the alarm threshold. This is referred to as an m-sample off-delay timer alarm configuration. Figures 4(b) and 4(c) show the alarms generated using a $0-$sample and $1-$sample on-delay timer configuration, respectively. Comparing Figures 4(b) and 4(c), it is clear that the $1-$sample delay-timer is able to reduce the rates of false and missed alarms. In fact, it is true that increasing the delay timer reduces the rates of the false and missed alarms. The industrial alarm standards set by the Engineering Equipment and Materials User Association (EEMUA)[17] and the International Society for Automation (ISA)[18] recommend values for the delay-timers based on the nature of the process variable. Table 1 provides suggested delay times for different process variables. Note that Table 1 only provides guidelines to design delay-timer alarms, but are by no means optimal for a given process variable. Thus for a delay-timer alarm configuration, the threshold limit and the delay time constitute the two main alarm design parameters. The optimal tuning for these alarm parameters for a given process is still an open problem. Apart from the (on/off) delay timers, other alarm configurations, such as the deadband[19] and the generalized delay timers[20] are also effective in dealing with complex process dynamics and noise sensitivities.

Contributions

The alarm design problem has received little attention so far from researchers in industry and academia. While the alarm design has been studied for linear, Gaussian, and stationary systems with uncorrelated signals,[20,21,22,23,24,25] the real systems often tend to be nonlinear, non-Gaussian and exhibit complex correlations in the dynamics. This is particularly true for a closed-loop system, since a closed system induces

strong system correlations even if the open-loop system has uncorrelated states. In this paper, we consider the alarm design problem for monitoring complex chemical processes represented by a stochastic nonlinear time-series model.

Given a stochastic nonlinear time-series model representation of a process, we are interested in designing a univariate delay timer alarm configuration for the process states. This is a challenging problem since: (1) the process can exhibit highly nonlinear behavior; (2) the state variables are not precisely known (due to modelling and discretization errors); and (3) the process states are not necessarily Gaussian, stationary or uncorrelated. The proposed method addresses the aforementioned issues to obtain a robust alarm design. The performance of the delay-timer is assessed based on the FAR and MAR rates. The conventional definitions for the FAR and MAR[26,27,3] – defined for Gaussian and stationary signals – are not applicable under the current settings, and are appropriately modified. Further, to ensure that the alarms are robust to any non-stationary process behavior, an expected and worst-case robust delay-timer alarm designs are proposed. Finally, the efficacy of the proposed alarm design is illustrated on a continuous stirred tank reactor (CSTR) reaction system. To the authors' best knowledge, none of the aforementioned challenges have been addressed previously in the context of alarm design.

Scope and Limitation

The proposed design is a model-based alarm design. It assumes that the process, for which the alarms are sought, can be represented using a time-series model representation. This limits the scope of the work to small processes or unit operations, in particular, for which such models are readily available or can be generated in a reasonable amount of time. Further, to ensure that the model is robust, we explicitly account for any modeling error, process uncertainties or noise. Further, the alarm design considered here is purely model-based and assumes limited access to the historical data. This makes the proposed alarm design method ideal in situations where the historical data is either unavailable or limited. For example, during the plant commissioning and start-up stage, or in the pharmaceutical manufacturing, where usually one or two campaign trials are performed before the current good manufacturing practice (cGMP) run. All these

scenarios are included within the scope of the current work. The notation is discussed next.

Notation: A random variable is denoted by X and its realization x. If a random variable $X \sim p(x)$ then X is distributed according to the probability density function (PDF) $p(x)$, such that $P(X \leq a)$ represents the probability of $X \leq a$. A sequence of a random variable is given by $X_{1:t} = \{X_1, \ldots, X_t\}$, where $X_1, \ldots X_t$ are random variables. $\mathbb{R}_+$, $\mathbb{P}$, and $\mathbb{N}$ denote the sets of non-negative reals in $\mathbb{R}$, the set of non-negative reals in the interval $[0, 1]$, and the set of integers, respectively. $\vee$ denotes a logical conjunction operator.

The remainder of the paper is organized as follows: the problem of alarm design is formally outlined first; the definition and design of a robust on-delay timer alarm configuration are discussed next; followed by the use of particle methods to evaluate the performance of the alarm system; and finally, the efficacy of the proposed robust alarm design is demonstrated on a simulation example.

Problem Statement

The alarm design problem addressed in this paper is formally stated in this section, but first we outline the process for which the alarms are sought. Let $X_t \in \mathcal{X} \subseteq \mathbb{R}^n$ describe a discrete-time, first-order Markov state process with initial density $X_0 \sim p(x_0)$ and a transition density $X_{t+1}|(X_t, U_t) \sim p(x_{t+1}|x_t, u_t)$, where $u_t \in \mathcal{U} \subseteq \mathbb{R}^p$ are exogenous control variables. To summarize, we have the following representation

Model 1. Stochastic nonlinear time-series model

$$X_0 \sim p(x_0), \tag{1a}$$

$$X_{t+1}|(X_t, U_t) \sim p(x_{t+1}|x_t, u_t), \tag{1b}$$

The densities in Model 1 are parametrized by $\theta \in \Theta \subseteq \mathbb{R}^k$. The set $\theta \in \Theta$ is assumed to be known, and thus for simplicity explicit dependency on θ is not shown. In situations, where θ is unknown, several methods are available to estimate the unknown parameters. For example,[28] provides a list of Bayesian and likelihood methods for parameter estimation in stochastic nonlinear time-series model. Finally, Model 1 represents a

general class of stochastic nonlinear time-series model. A sub-class of Model 1, considered in this paper is defined as follows

Model 2. Stochastic nonlinear, non-Gaussian model

$$X_0 \sim p(x_0), \tag{2a}$$

$$X_{t+1} = f_t(X_t, U_t, V_t), \tag{2b}$$

where $f_t : \mathbb{R}^n \times \mathbb{R}^p \times \mathbb{R}^n \to \mathbb{R}^n$ is an n-dimensional state transition function and $V_t \in \mathbb{R}^n$ is the state noise sequence.

Many unit operations (e.g, reactors, distillation columns; dryers) can be represented by Model 2. For example, the concentrations of species inside an isothermal continuous stirred tank reactor (CSTR) can be represented as given below

Example 1. (Semibatch Reactor) The concentration of n species, denoted by $X_t \in \mathbb{R}^n$, in an isothermal CSTR of constant volume $\gamma \in \mathbb{R}_+$ with initial concentration $X_0 \sim p(x_o)$, and flow rates $U_t \in \mathbb{R}^p$ can be modeled as follows

$$f_t(X_t, U_t, V_t) \equiv Sr(X_t) + \frac{1}{\gamma} G U_t - \frac{1}{\gamma} \mathbf{1}^{\mathrm{T}} U_t X_t + V_t, \tag{3a}$$

where: $S \in \mathbb{R}^{n \times q}$ and $G \in \mathbb{R}^{n \times p}$ are the stoichiometric and volumetric concentration matrices, respectively, with q denoting the number of independent reactions, and $\mathbf{1}_p$ is a vector of ones of dimension p; the vector $r : \mathbb{R}^n \to \mathbb{R}^q$ is the rate function; and $V_t \in \mathbb{R}^n$ is the additive state noise sequence.

Definition 1. (Proper Signal) A signal $\{Z_t\}_{t \in \mathbb{N}}$ is proper if there exists a $t_\beta \in \mathbb{N}$ such that $\{Z_t\}_{t \in \mathbb{N}}$ for all $t \leq t_\beta$ represents normal operations and $\{Z_t\}_{t \in \mathbb{N}}$ for all $t > t_\beta$ represents abnormal operations.

Definition 1 assumes that a proper signal starts in the normal operating region and in finite time transitions into the abnormal operating region. The assumed order of process operation in Definition 1 is strictly for mathematical convenience and has no bearing on the material presented here. We make the following assumptions on Model 2

Assumption 1. $\{V_t\}_{t\in\mathbb{N}} \in \mathbb{R}^n$ is a sequence of independent random variables distributed according to $V_t \sim p(v_t)$, and defined independent of $X_0 \sim p(x_0)$.

Assumption 2. $p(x_0)$ and $p(v_t)$ are known in their classes (e.g., Gaussian, uniform, Rayleigh) and are parametrized by finite number of moments (e.g., mean, variance).

Problem 1. For a process represented by Model 2 under Assumptions 1 and 2, design a univariate delay timer for the process state $\{X_t\}_{t\in\mathbb{N}}$ using a proper input signal $\{U_t\}_{t\in\mathbb{N}}$.

Problem 1 assumes that a proper input signal is available for designing the alarm system. Here, the input sequence is proper in the sense defined in Definition 1. In practical settings, a proper input signal can be constructed based on process knowledge or process design. More on the use of proper input signal is discussed later. In Problem 1, Assumptions 1 and 2 are the regulatory conditions that allow for the simulation of Model 2 for a given input signal. Finally, the simplifying assumptions on the Gaussianity, stationarity, or uncorrelated nature of the states in Model 2 are not made in this paper, which are the standard assumptions in most of the existing work on alarm design.[26,23]

On-Delay Timer Alarm Configuration

A limit-checking alarm generation method raises an alarm every time a process variable $\{X_t\}_{t\in\mathbb{N}}$ exceeds certain predetermined threshold limit. If $A_t \in \{0,1\}$ denotes the state of the alarm, then $A_t = 0$ represents the "off" state and $A_t = 1$ represents the "on" state. Assuming $n = 1$, a limit-checking method generates an alarm sequence $\{A_t\}_{t\in\mathbb{N}}$ as follows

$$A_t \equiv \begin{cases} 1 & \text{if } X_t \geq S_x \text{ (or } X_t \leq S_x) \\ 0 & \text{otherwise} \end{cases}, \tag{4}$$

where $S_x \in \mathbb{R}$ is the alarm trip point. Similarly, for $n \geq 2$ alarms are generated by defining (4) for each state. Here we only consider a univariate alarm design, where the objective is to design an alarm system for a single state in Model 2. Now without the loss of generality, only one-sided univariate alarm design is considered here that is raised when $X_t \geq S_x$. Now based on how the alarm generation mechanism in (4)

is implemented, a host of alarm configurations, such as deadband,[3] delay timers[29] and generalized delay timers[20] can be studied and designed.

A delay timer alarm configuration, also called a debounce timer alarm configuration is preferred in industries for its simplicity. Intuitively, the human beings prefer to wait for a while before reacting to any abnormality to avoid any temporary over or under reaction. A delay timer uses the same principle to minimize the operator reaction to unknown process disturbances and process noise.[3] For example, an n_x-sample on-delay timer triggers only after $\{X_t\}_{t\in\mathbb{N}}$ is continuously over S_x for at least n_x samples. For an n_x-sample on-delay timers, if the system returns back to the normal operations before n_x samples, the alarm is not activated. Similarly, once an alarm is raised, it will be cleared right away if one sample goes below the alarm trip point. Mathematically, if $\bar{A}_t \in \{0,1\}$ denotes the state of the alarm for an n_x-sample on-delay timer, then $\{\bar{A}_t\}_{t\in\mathbb{N}}$ is generated as follows

$$\bar{A}_t \equiv \begin{cases} 1 & \text{if } X_{t-n_x} \geq S_x \vee, \ldots, \vee X_t \geq S_x \\ 0 & \text{otherwise} \end{cases} . \tag{5}$$

It is easy to see that for $n_x = 0$, $\bar{A}_t = A_t$ for all $t \in \mathbb{N}$. Similarly, in the case of an m_x-sample off-delay alarm configuration, once an alarm is raised it is cleared only when $\{X_t\}_{t\in\mathbb{N}}$ is continuously under S_x for m_x consecutive samples. In this paper we only consider the design of an n_x-sample on-delay timer alarm configuration, but can be extended to include an m_x-sample off-delay alarm configuration. Based on the alarm generation mechanism in (5), it is clear that for an on-delay timer, n_x and S_x are the two main alarm design parameters. An appropriate choice of (n_x, S_x) is critical for it affects the performance of the alarm configuration. The design of (n_x, S_x) for a univariate on-delay timer is discussed next.

Design and Assessment of On-Delay Timers

For an on-delay timer alarm configuration, a poor choice of (n_x, S_x) results in two types of misclassified alarm errors – false positive (or false alarm) and false negative (or missed alarm). A false alarm is an alarm that is raised while $\{X_t\}_{t\in\mathbb{N}}$ is still in normal operations, and a missed alarm occurs when the alarm is not raised even when $\{X_t\}_{t\in\mathbb{N}}$ is behaving abnormally. The performance of an on-delay timer alarm system

through the use of a receiver operating characteristic (ROC) curve is discussed next.

ROC-based Alarm Design

The FAR and MAR provide a reliable measure of the accuracy of a univariate alarm system design. Assuming that the FAR and MAR for an n_x-sample on-delay timer alarm is known, the accuracy of the alarm system can be graphically represented through a receiver operating characteristic (ROC) curve.[22] In statistics, an ROC curve is a graphical plot illustrating the performance of a binary classifier system. The ROC curve is created by plotting the true positive rate against the false positive rate as the discrimination threshold is varied. The use of ROC curves in alarm design was first introduced in,[22] where the true positive rate was replaced by the missed alarm rate. Therefore, an ROC curve for a univariate alarm system captures the trade-off between the FAR and MAR as S_x is varied in $\mathbb{R}$. A schematic of an ROC curve for an n_x-sample on-delay timer alarm configuration obtained for different n_x values as S_x is varied, as shown in Figure 5.

It is possible to choose $(n_x, S_x) \in \mathbb{N} \times \mathbb{R}$ directly from the ROC curve in Figure 5. This is achieved by choosing the alarm parameters in the set $(n_x, S_x) \in \mathbb{N} \times \mathbb{R}$ one at a time. For example, the EEMUA and ISA recommend nominal values for the delay timers based on the nature of the process variable (see Table 1). Based on these guidelines, n_x can be fixed a priori, and an optimal S_x found by varying $S_x \in \mathbb{R}$ until an acceptable FAR and MAR is achieved (see Figure 5 for illustration). Typically, these acceptable FAR and MAR values are decided by the process safety engineers and are usually available a priori. This approach to alarm design is referred to as the ROC-based alarm design. The ROC-based alarm design can also be implemented by keeping S_x fixed, and varying $n_x \in \mathbb{N}$ until the desired FAR and MAR are achieved.

Normal and Abnormal Operations

The definitions of FAR and MAR are based on the clear understanding of the process behavior in the normal and abnormal operating conditions. Specifically, we are interested in characterizing the normal and abnormal operations of a process state $\{X_t\}_{t\in\mathbb{N}}$. First, note that it is plausible to define such regimes since $\{X_t\}_{t\in\mathbb{N}}$ is a proper signal. This is because simulating Model 2 with a proper input signal $\{U_t\}_{t\in\mathbb{N}}$ yields a

proper state signal $\{X_t\}_{t\in\mathbb{N}}$.

One approach to construct a probabilistic representation of the normal and abnormal operations of a process variable is to use the measurements. In fact several parametric and non-parametric change-detection algorithms, such as Shewhart chart, moving average charts, cumulative sum procedures, generalized likelihood ratio test, Bayesian and information criterion approaches can be used to detect multiple change-points within a signal.[30,31] Once the multiple change-points are detected, the data can be classified into the normal or abnormal process behavior based on prior process information. Once all the different sections of a signal have been classified, a histogram method can be used to find the probability density functions (PDFs) of the underlying normal and abnormal operations.[23] Of course this last step assumes that the signal in the normal and abnormal regions are individually independent and identically distributed stationary signal.[23,26,27] For example, Figure 6 shows a schematic of the PDFs under normal and abnormal operations for the variable in Figure 4(a). The PDFs in Figure 6 are constructed assuming that the signal in Figure 4(a) is independent and identically distributed stationary signal under both normal and abnormal operations (see Figure 4(a) for details).

Despite the success with existing methods in characterizing the normal and abnormal operations, under the current settings, existing methods are not applicable since $\{X_t\}_{t\in\mathbb{N}}$ is non-stationary. In fact, even if the change-points for $\{X_t\}_{t\in\mathbb{N}}$ are known (assuming $\{X_t\}_{t\in\mathbb{N}}$ is measured), a histogram method can not be used to construct the PDFs for $\{X_t\}_{t\in\mathbb{N}}$ under the normal and abnormal operations (since $\{X_t\}_{t\in\mathbb{N}}$ is non-stationary). To address these limitations, we propose the use of Model 2 to construct the PDFs for $\{X_t\}_{t\in\mathbb{N}}$ under the normal and abnormal process operations.

Assumption 3. The time of fault $t_\beta \in \mathbb{N}$ is known such that $\{X_t\}_{t\in\mathbb{N}}$ is in normal operations for $t \in \{0,1,\ldots,t_\beta-1\}$ and in abnormal operations for $t \in \{t_\beta, t_\beta+1,\ldots,t_N\}$, where $t_N \in \mathbb{N}$ denotes the fixed time-length of the signal.

In Assumption 3 the time of fault is assumed to be known a priori; however, in practice, this may not be true. In fact, the objective of any FDD system is to compute the magnitude and time of occurrence of a fault. Since this paper only addresses the problem of alarm design, and not that of an FDD system, we

will assume that the time of fault is known a priori. Further in Assumption 3, we consider that the process starts normally at $t = 0$ but transits into the abnormal region at time $t = t_\beta$. It also assumes that there is only a single transition from the normal to abnormal operation in the time horizon $t \in \{0, \ldots, t_N\}$.

Observe that for a process described by Model 2, the density function $p(x_t)$ provides a suitable probabilistic representation of the state $\{X_t\}_{t\in\mathbb{N}}$. In other words, the PDF $p(x_t)$ encompasses all statistical information about $\{X_t\}_{t\in\mathbb{N}}$ under the normal and abnormal operations. Now under Assumption 3, $p(x_t)$ can be decomposed as follows

$$p(x_t) = \begin{cases} p_N(x_t) & \text{for } t = 0, \ldots, t_\beta - 1, \\ p_F(x_t) & \text{for } t = t_\beta, \ldots, t_N, \end{cases} \tag{6}$$

where $X_t \sim p_N(\cdot)$ and $X_t \sim p_F(\cdot)$ represent the PDFs of $\{X_t\}_{t\in\mathbb{N}}$ under the normal and abnormal operations, respectively. For now, $p_N(\cdot)$ and $p_F(\cdot)$ in (6) are assumed to be known; however, later we describe a sequential particle approach to approximate $p_N(\cdot)$ and $p_F(\cdot)$ via simulation of Model 2. Finally, a schematic of $p_N(\cdot)$ and $p_F(\cdot)$ are shown in Figure 7. Note that the PDFs in Figure 7 are strictly shown for illustrative purposes to highlight that the current framework supports non-Gaussian distributions as well. This is a significant departure from the existing work on alarm design where the PDFs under the normal and abnormal operations are assumed to be Gaussian (see Figure 6, for example).

FAR and MAR Calculations

Given a probabilistic representation of $\{X_t\}_{t\in\mathbb{N}}$ under the normal and abnormal operations in (6), let $F_t(n_x, S_x)$ and $M_t(n_x, S_x)$ denote the FAR and MAR for an n_x-sample on-delay timer alarm system, respectively. Here $(n_x, S_x) \in \mathbb{N} \times \mathbb{R}$ are the alarm parameters that need to be designed.

As discussed earlier, for $n_x = 0$, the rate of false alarm $F_t(0, S_x)$ for a 0-sample on-delay timer alarm system is the Type 1 error committed in raising the alarm under normal operations the moment $X_t \geq S_x$. Intuitively, $F_t(0, S_x)$ is defined as the area under the PDF $p_N(\cdot)$ for X_t greater than S_x (see Figure 7 for

illustration). Mathematically, we define $F_t(0, S_x)$ as follows

$$F_t(0, S_x) \equiv \mathbb{P}_N(X_t > S_x) = \int_{S_x}^{+\infty} p_N(dx_t), \tag{7}$$

where $p_N(dx_t) \equiv p_N(x_t)dx_t$ is the probability distribution of $\{X_t\}_{t\in\mathbb{N}}$ under normal operations. Similarly, for a 0-sample on-delay timer alarm system, the rate of missed alarm $M_t(0, S_x)$ is the Type II error committed by not raising the alarm for $X_t < S_x$ under abnormal operations. In other words, $M_t(n_x, S_x)$ is the area under the PDF $p_F(\cdot)$ for X_t less than S_x (see Figure 7). Similar to (7), $M_t(n_x, S_x)$ can be mathematically defined as follows

$$M_t(0, S_x) \equiv \mathbb{P}_F(X_t < S_x) = \int_{-\infty}^{S_x} p_F(dx_t), \tag{8}$$

where $p_F(dx_t) \equiv p_F(x_t)dx_t$ is the probability distribution of $\{X_t\}_{t\in\mathbb{N}}$ under the abnormal operations. It is clear from the FAR and MAR expressions in (7) and (8) that lowering the alarm threshold S_x reduces the probability of missed alarms but increases the probability of false alarms, and vice verse. See Figure 7 for illustration.

Now extending the definitions of FAR and MAR in (7) and (8) for an n_x-sample on-timer delay alarm system, we can define the rate of false alarm $F_t(n_x, S_x)$ as the Type I error committed in raising the alarm after n_x continuous samples satisfy the condition $X_t \geq S_x$ in the normal operating regime. Assuming $n_x < t_\beta$ the rate of false alarms for an n_x-sample on-timer delay alarm can be defined as

$$F_t(n_x, S_x) \equiv \mathbb{P}_N(X_{t-n_x} \geq S_x, \ldots, X_t \geq S_x) = \tag{9}$$

$$\begin{cases} 0 & \text{for } t = 0, \ldots, n_x - 1 \\ \underbrace{\int_{S_x}^{+\infty} \cdots \int_{S_x}^{+\infty}}_{n_x+1 \text{ terms}} p_N(dx_{t-n_x:t}), & \text{for } t = n_x, \ldots, t_\beta - 1 \end{cases},$$

for all $S_x \in \mathbb{R}$. In (9), $p_N(dx_{t-n_x:t}) \equiv p_N(x_{t-n_x:t})dx_{t-n_x:t}$ is the joint probability distribution function for the random sequence $X_{t-n_x:t} \equiv \{X_{t-n_x}, X_{t-n_x+1,\ldots,X_t}\}$ under the normal operations. Note that for an n_x-sample on-timer delay alarm system, since an alarm is raised only after all n_x continuous samples have satisfied the condition $X_t \geq S_x$, there are no false alarms for the $n_x - 1$ continuous samples satisfying $X_t \geq S_x$

in the normal operating regime. Thus for any $n_x \in \mathbb{N}$, we have $F_t(n_x, \cdot) = 0$ for all $t = 0, \ldots, n_x - 1$ (see (9)). Now observe that for $n_x = 0$, the rate of false alarms $F_t(0, S_x)$ in (9) is same as (7) for all $S_x \in \mathbb{R}$. Similarly, for an n_x-sample on-timer delay alarm configuration, the rate of missed alarm $M_t(n_x, S_x)$ is defined as the Type II error committed in not raising the alarm since n_x continuous samples satisfy the condition $X_t < S_x$ in the abnormal operating regime. Assuming $t_\beta + n_x < t_N$, the MAR for an n_x-sample on-timer delay alarm can be defined as follows

$$M_t(n_x, S_x) \equiv \mathbb{P}_F(X_{t-n_x} < S_x, \ldots, X_t < S_x) = \tag{10}$$

$$\begin{cases} 1 & \text{for } t = t_\beta, \ldots, t_\beta + n_x - 1 \\ \underbrace{\int_{-\infty}^{S_x} \cdots \int_{-\infty}^{S_x}}_{n_x+1 \text{ terms}} p_F(dx_{t-n_x:t}) & \text{for } t = t_\beta + n_x, \ldots, t_N \end{cases},$$

for all $S_x \in \mathbb{R}$. In (10), $p_F(dx_{t-n_x:t}) \equiv p_N(x_{t-n_x:t})dx_{t-n_x:t}$ is the joint probability distribution function for the random sequence $X_{t-n_x:t} \equiv \{X_{t-n_x}, X_{t-n_x+1,\ldots,X_t}\}$ under the abnormal operations. Observe that for an n_x-sample on-timer delay alarm configuration, if an alarm is raised after n_x continuous samples satisfy the condition $X_t \geq S_x$, we still miss the alarms for the $n_x - 1$ continuous samples satisfying $X_t \geq S_x$ in the abnormal operating regime. Thus for any $n_x \in \mathbb{N}$, we have $M_t(n_x, \cdot) = 1$ for all $t = t_\beta, \ldots, t_\beta + n_x - 1$ (see (10)). Finally, observe that the rate of missed alarm in (10) for $n_x = 0$ is same as (8).

Observe that the FAR and MAR for an n_x-sample on-delay timer defined in (9) and (10), respectively, are time-varying. This is because Model 2 represents a non-stationary process model. In other words, for any $(n_x, S_x) \in \mathbb{N} \times \mathbb{R}$, the joint density functions – $p_N(x_{t-n_x:t})$ in (9) and $p_F(x_{t-n_x:t})$ in (10) – need to be computed for each sampling time $t \in \mathbb{N}$. Figure 8 shows a schematic of the density functions p_N and p_F under the normal and abnormal operations. It is clear from Figure 8 that the density functions not only exhibit non-i.i.d. behavior, but are in fact also non-stationary and non-Gaussian. This poses a unique challenge as existing histogram-based methods can not be used to compute the FAR and MAR in (9) and (10), respectively, as these methods explicitly require $\{X_t\}_{t\in\mathbb{N}}$ to be an i.i.d. sequence.[26]

Observe that although the FAR and MAR in (9) and (10), respectively, are defined for a non-stationary process, it can also be used under a stationary process conditions. Assuming $2n_x < t_\beta - 1$ and for any

$\tau \in \{2n_x, \ldots, t_\beta - 1\}$, the FAR in (9) under stationary normal operations simplifies as follows

$$F_t(n_x, S_x) = \begin{cases} 0 & \text{for } t = 0, \ldots, n_x - 1 \\ \\ K_N & \text{for } t = n_x, \ldots, t_\beta - 1 \end{cases}, \tag{11}$$

where

$$K_N = \underbrace{\int_{S_x}^{+\infty} \cdots \int_{S_x}^{+\infty}}_{n_x+1 \text{ terms}} p_N(dx_{\tau-n_x:\tau}),$$

for all $S_x \in \mathbb{R}$. Observe that the joint density function in (11) is time-invariant for all $(n_x, S_x) \in \mathbb{N} \times \mathbb{R}$. Similarly, assuming $t_\beta + 2n_X \leq t_N$, for any $\gamma \in \{t_\beta + 2n_X, \ldots, t_N\}$ the MAR in (10) under stationary abnormal operations simplifies to

$$M_t(n_x, S_x) = \begin{cases} 1 & \text{for } t = t_\beta, \ldots, t_\beta + n_x - 1 \\ \\ K_F & \text{for } t = t_\beta + n_x, \ldots, t_N \end{cases}, \tag{12}$$

where

$$K_F = \underbrace{\int_{-\infty}^{S_x} \cdots \int_{-\infty}^{S_x}}_{n_x+1 \text{ terms}} p_F(dx_{\gamma-n_x:\gamma}),$$

for all $S_x \in \mathbb{R}$. Thus (11) and (12) highlight that the FAR and MAR definitions in (9) and (10), respectively, are generic and can be used under the stationary and non-stationary process normal and abnormal process operations. Finally, note that no Gaussianity or other simplifying assumptions are made on the underlying density functions in (9) and (10) or (11) and (12).

Robustness

The FAR and MAR in (9) and (10) can be used with the ROC-based method (see Section c) to select an optimal parameter set $(n_x, S_x) \in \mathbb{N} \times \mathbb{R}$ for an n_x-sample on-timer delay timer alarm configuration. Despite the simplicity of the design method, observe that for a time-varying FAR and MAR in (9) and (10), respectively, the parameter set $(n_x, S_x) \in \mathbb{N} \times \mathbb{R}$ needs to be designed at each $t \in \mathbb{N}$. In other words, the time-varying FAR and MAR yields an ROC curve that is also time-varying. Note that designing an alarm

system at each sampling time is not only impractical, it may lead to serious process upsets and unsafe process operations. Observe that this time-varying alarm design problem arises due to the time-varying FAR and MAR in (9) and (10), respectively. One approach to make the alarm systems robust to any non-stationary process disturbances and fluctuations is to consider the following robust definitions of FAR and MAR

$$F^E(n_x, S_x) = \frac{1}{(t_\beta - 1 - n_x)} \sum_{t=n_x}^{t_\beta - 1} F_t(n_x, S_x), \tag{13a}$$

$$M^E(n_x, S_x) = \frac{1}{(t_N - t_\beta - n_x)} \sum_{t=t_\beta + n_x}^{t_N} M_t(n_x, S_x), \tag{13b}$$

where $F^E(n_x, S_x)$ and $M^E(n_x, S_x)$ are the expected-case FAR and MAR, respectively. Observe that (13a) and (13b) are time-invariant and robust to any non-stationary process behavior. Also, since $F_t(n_x, S_x) = 0$ for $t = 0, \ldots, n_x - 1$ and $M_t(n_x, S_x) = 1$ for $t = t_\beta, \ldots, t_\beta + n_x - 1$ (see (9), and (10), respectively), these terms are not used in the calculations (see (13a) and (13b)). This ensures that the expected FAR and MAR are not biased for large $n_x \in \mathbb{N}$ values.

The new FAR and MAR definitions in (13a) and (13b) can also be used in the expected-case ROC-based alarm design. This is done by using (13a) and (13b) to construct an ROC curve. Note that while the FAR and MAR in (13a) and (13b) yield an expected-case alarm design, it is also possible to formulate a worst-case alarm design by considering the following definitions for the FAR and MAR

$$F^W(n_x, S_x) = \max_{t \in \{n_x, \ldots, t_\beta - 1\}} F_t(n_x, S_x), \tag{14a}$$

$$M^W(n_x, S_x) = \max_{t \in \{t_\beta + n_x, \ldots, t_N\}} M_t(n_x, S_x), \tag{14b}$$

where $F^W(n_x, S_x)$ and $M^W(n_x, S_x)$ are the worst-case FAR and MAR, respectively. Again, the worst-case alarm design can be performed by computing the ROC curve using the worst-case FAR and MAR in (14a) and (14b). In summary, the new FAR and MAR definitions in (13a) – (13b) and (14a) – (14b) yield an expected-case and worst-case alarm designs, respectively. In the next section, a sequential particle method is discussed to compute the FAR and MAR.

Particle Methods

The computation of the FAR and MAR in (13a) – (13b) and (14a) – (14b), respectively, require the density functions p_N and p_F under the normal and abnormal operations to be known a priori; however, in practice, this is rarely true and often need to be estimated from data. Now as discussed earlier, the non-stationary process behavior exhibited by $\{X_t\}_{t\in\mathbb{N}}$ limits the use of data-based methods discussed in.[26,23] In this paper, we propose to calculate p_N and p_F using Model 2 directly. This is done as follows. First note that using the Law of Total Probability, the density function p_N, for example, can be written as follows

$$p_N(x_t) = \int p(x_t, x_{t-1})dx_{t-1}, \tag{15a}$$

$$= \int p(x_t|x_{t-1})p_N(dx_{t-1}), \tag{15b}$$

where $p(x_t|x_{t-1})$ is the state transition density in Model 2 and $p_N(dx_{t-1}) \triangleq p_N(x_{t-1})dx_{t-1}$ is a distribution function for $\{X_t\}_{t\in\mathbb{N}}$ under the normal process operations. Now for a given $p_N(x_{t-1})$, equation (15b) provides a recursive approach to compute $p_N(x_t)$ for all $t \in \mathbb{N}$ using Model 2 directly. Similarly, using the Law of Total Probability, p_F can be recursively written as follows

$$p_F(x_t) = \int p(x_t, x_{t-1})dx_{t-1}, \tag{16a}$$

$$= \int p(x_t|x_{t-1})p_F(dx_{t-1}), \tag{16b}$$

where $p_F(dx_{t-1}) \triangleq p_F(x_{t-1})dx_{t-1}$ is the distribution function for $\{X_t\}_{t\in\mathbb{N}}$ under abnormal process operations. Note that while Model 2 provides a recursive approach to calculate p_N and p_F, the densities in (15b) and (16b) do not lend themselves to any closed-form solutions for the representation for the choice of model in Model 2. This is because (15b) and (16b) involve integration with respect to complex non-Gaussian density functions (recall that the densities in Model 2 are both nonlinear and non-Gaussian).

To address this problem, we propose the use of a sequential Monte-Carlo or particle method[32,28] to approximate p_N and p_F in (15b) and (16b), respectively, to arbitrary accuracy. A particle method is a recursive approach that approximates the density functions in (15b) and (16b) by propagating a set of 'particles' generated from the previous sampling time. For the sake of brevity, we assume that the readers

are familar with the theory of particle methods. For a detailed exposition on particle methods the reader is referred to a recently published tutorial on this subject.[33]

The particle approximation of p_N in (15b) is given as follows. Assume we have M-i.i.d. random particles, denoted by $\{X_{t-1}^i\}_{i=1}^M \sim p_N(x_{t-1})$, and distributed according to $p_N(x_{t-1})$ then the distribution function of X_{t-1} can be approximately defined as follows

$$\tilde{p}_N(dx_{t-1}) = \frac{1}{M}\sum_{i=1}^{M} \delta_{X_{t-1}^i}(dx_{t-1}), \tag{17}$$

where $\tilde{p}_N(dx_{t-1})$ is an M-particle approximation of the distribution function $p_N(dx_{t-1})$, and $\delta_X(dx)$ is a Dirac delta measure centered at particle X. In (17), the particle method approximates the distribution function of X_{t-1} using a sum of M Dirac delta measures, each centered around M random samples distributed according to $p(x_{t-1})$. Now, substituting (17) into (15b) yields

$$\tilde{p}_N(x_t) = \int p_N(x_t|x_{t-1}) \frac{1}{M}\sum_{i=1}^{M} \delta_{X_{t-1}^i}(dx_{t-1}), \tag{18a}$$

$$= \frac{1}{M}\sum_{i=1}^{M} \int p(x_t|x_{t-1}) \delta_{X_{t-1}^i}(dx_{t-1}), \tag{18b}$$

$$= \frac{1}{M}\sum_{i=1}^{M} p(x_t|X_{t-1}^i), \tag{18c}$$

where the last equality results from the integral property of the Dirac delta measure. Observe that in (18c), the density function $p_N(x_t)$ is approximated using a sum of M state transition functions, $p_N(x_t|X_{t-1}^i)$, where $i = 1, \ldots, M$. Now since the M transition functions in (18c) are equally weighted (each has a weight M^{-1}), we can generate M random particles $\{X_t^i\}_{i=1}^M \sim p_N(x_t)$, distributed according to $p_N(x_t)$ by simply passing each particle in the set $\{X_{t-1}^i\}_{i=1}^M$ through the state transition function. Now if $\{X_t^i\}_{i=1}^M \sim p_N(x_t)$ denotes a particle set generated using (17) and distributed according to the density function $p_N(x_t)$ then the distribution function $p_N(dx_t)$ can be approximately represented as follows

$$\tilde{p}_N(dx_t) = \frac{1}{M}\sum_{i=1}^{M} \delta_{X_t^i}(dx_t), \tag{19}$$

where $\tilde{p}_N(dx_t)$ is an M-particle approximation of $p_N(dx_t)$. Similarly if $\{\bar{X}_{t-1}^i\}_{i=1}^M \sim p_F(x_{t-1})$ represents a set of M-i.i.d. particles distributed according to $p_F(x_{t-1})$, then random particles from the density function

$p_F(x_t)$ can be generated using the relation in (16b) such that

$$\tilde{p}_F(x_t) = \frac{1}{M}\sum_{i=1}^{M} p(x_t|\bar{X}_{t-1}^i), \tag{20}$$

where $\tilde{p}_F(dx_t)$ is an M-particle approximation of $p_F(dx_t)$. Finally, if $\{\bar{X}_t^i\}_{i=1}^M \sim p_F(x_t)$ represents a particle set generated using (20) and distributed according to $p_F(x_t)$ then the distribution function $p_F(dx_t)$ can be approximated as

$$\tilde{p}_F(dx_t) = \frac{1}{M}\sum_{i=1}^{M} \delta_{\bar{X}_t^i}(dx_t), \tag{21}$$

where $\tilde{p}_F(dx_t)$ is an M-particle approximation of $p_F(dx_t)$. Now having computed a particle approximation of the density functions p_N and p_F in (19) and (21), respectively, next we discuss the particle approximation of the FAR and MAR in (9) and (10), respectively.

Particle Approximations of FAR and MAR

As discussed earlier, for the choice of model in Model 2, no closed form solutions exist to the FAR and MAR in (9) and (10), and therefore need to be approximated. In this section, we extend the use of particle method, discussed earlier to approximate the FAR and MAR using the particle approximations of p_N and p_F computed in (19) and (21), respectively. First note that the FAR in (9) for all $t \in \{n_x, \ldots, t_\beta - 1\}$ is given by

$$F_t(n_x, S_x) = \underbrace{\int_{S_x}^{+\infty} \cdots \int_{S_x}^{+\infty}}_{n_x+1 \text{ terms}} p_N(dx_{t-n_x:t}). \tag{22}$$

It is clear that the FAR in (22) involves a complex multidimensional integral with respect to the joint distribution $p_N(dx_{t-n_x:t})$. Now computing a particle approximation of (22) first requires a particle approximation of the joint distribution function. This is achieved as follows – first by appealing to the conditional probability and using the Markov structure of Model 2, the joint distribution $p_N(dx_{t-n_x:t})$ in (22) can be rewritten as follows

$$p_N(dx_{t-n_x:t}) = p(dx_t|x_{t-1})p_N(dx_{t-n_x:t-1}). \tag{23}$$

Similarly, by repeatedly appealing to the conditional probability, (23) can further be decomposed and rewritten as follows

$$p_N(dx_{t-n_x:t}) = p_N(dx_{t-n_x}) \prod_{i=t-n_x+1}^{t} p(dx_i|x_{i-1}). \tag{24}$$

Equation (24) decomposes an n_x-dimensional joint distribution function as a product of n_x one-dimensional distribution functions. Now as discussed in (19), if the particle approximation of the distribution $p_N(dx_{t-n_x})$ is given by

$$\tilde{p}_N(dx_{t-n_x}) = \frac{1}{M}\sum_{j=1}^{M} \delta_{X^j_{t-n_x}}(dx_{t-n_x}), \tag{25}$$

where $\{X^j_{t-n_x}\}_{j=1}^M \sim p_N(x_{t-n_x})$ is distributed according to $p_N(x_{t-n_x})$ then substituting (25) into (24) yields

$$\tilde{p}_N(dx_{t-n_x:t})$$

$$= \frac{1}{M}\sum_{j=1}^{M} \delta_{X^j_{t-n_x}}(dx_{t-n_x}) \left[\prod_{i=t-n_x+1}^{t} p_N(dx_i|x_{i-1})\right], \tag{26a}$$

$$= \frac{1}{M}\sum_{j=1}^{M} \left[\prod_{i=t-n_x+1}^{t} p_N(dx_i|X^j_{i-1})\right] \delta_{X^j_{t-n_x}}(dx_{t-n_x}), \tag{26b}$$

where $\tilde{p}_N(dx_{t-n_x:t})$ is an M-particle approximation of the joint distribution function $p_N(dx_{t-n_x:t})$. Now given (26b), random particles from $p_N(dx_{t-n_x:t})$ can be generated by passing each particle in the set $\{X^j_{t-n_x}\}_{j=1}^M$ consecutively n_x times though the state equation. Now if $\{X^j_{t-n_x:t}\}_{j=1}^M \sim p_N(x_{t-n_x:t})$ denotes a particle set generated from (26b) and distributed according to $p_N(x_{t-n_x:t})$ then we can write

$$\tilde{p}_N(dx_{t-n_x:t}) = \frac{1}{M}\sum_{j=1}^{M} \delta_{X^j_{t-n_x:t}}(dx_{t-n_x:t}). \tag{27}$$

Finally, substituting (27) into (22) yields

$$\tilde{F}_t(n_x, S_x)$$

$$= \underbrace{\int_{S_x}^{+\infty} \cdots \int_{S_x}^{+\infty}}_{n_x+1 \text{ terms}} \frac{1}{M}\sum_{j=1}^{M} \delta_{X^j_{t-n_x:t}}(dx_{t-n_x:t}), \tag{28a}$$

$$= \frac{1}{M}\sum_{j=1}^{M} \underbrace{\int_{S_x}^{+\infty} \cdots \int_{S_x}^{+\infty}}_{n_x+1 \text{ terms}} \delta_{X^j_{t-n_x:t}}(dx_{t-n_x:t}), \tag{28b}$$

$$= \frac{1}{M}\sum_{j=1}^{M} \mathbf{1}_{\Omega}(X^j_{t-n_x:t}), \tag{28c}$$

where $\tilde{F}_t$ is an M-particle approximation of F_t and $\mathbf{1}_\Omega : \mathbb{R}^{n_x+1} \to \{0,1\}$ is an indicator function defined over a set $\Omega \subset \mathbb{R}^{n_x+1}$ such that

$$\mathbf{1}_\Omega(X^j_{t-n_x:t}) = \begin{cases} 1 & \text{if } X^j_{t-n_x:t} \in \Omega \\ 0 & \text{otherwise} \end{cases}, \tag{29}$$

and $\Omega \triangleq [S_x, +\infty)^{n_x+1}$. Thus as shown in (28c), the proposed method approximates the FAR in (9) as the average of M indicator functions defined over the set Ω. Further, as one would expect, the maximum probability of false alarms, as computed in (28c) is one, which corresponds to the condition $X^j_{t-n_x:t} \in \Omega$ for all $j = 1, \ldots, M$.

Similarly, computing a particle approximation of the MAR in (10) entails computing an approximation to

$$M_t(n_x, S_x) = \underbrace{\int_{-\infty}^{S_x} \cdots \int_{-\infty}^{S_x}}_{n_x+1 \text{ terms}} p_F(dx_{t-n_x:t}), \tag{30}$$

for all $t \in \{t_\beta + n_x, \ldots, t_N\}$. If $\{\bar{X}^j_{t-n_x:t}\}_{j=1}^M \sim p_F(x_{t-n_x:t})$ represents a set of particles distributed according to $p_F(x_{t-n_x:t})$ then for all $t \in \{t_\beta + n_x, \ldots, t_N\}$ we have

$$\tilde{p}_F(dx_{t-n_x:t}) = \frac{1}{M} \sum_{j=1}^{M} \delta_{\bar{X}^j_{t-n_x:t}}(dx_{t-n_x:t}), \tag{31}$$

where $\tilde{p}_F(dx_{t-n_x:t})$ is an M-particle approximation of $p_F(dx_{t-n_x:t})$. Now substituting (31) into (30) yields

$$\begin{aligned} &\tilde{M}_t(n_x, S_x) \\ &= \underbrace{\int_{-\infty}^{S_x} \cdots \int_{-\infty}^{S_x}}_{n_x+1 \text{ terms}} \frac{1}{M} \sum_{j=1}^{M} \delta_{\bar{X}^j_{t-n_x:t}}(dx_{t-n_x:t}), && \text{(32a)} \\ &= \frac{1}{M} \sum_{j=1}^{M} \mathbf{1}_{\mathbb{R}\setminus\Omega}(\bar{X}^j_{t-n_x:t}), && \text{(32b)} \end{aligned}$$

where $\tilde{M}_t$ is an M-particle approximation of M_t and

$$\mathbf{1}_{\mathbb{R}\setminus\Omega}(\bar{X}^j_{t-n_x:t}) = \begin{cases} 1 & \text{if } \bar{X}^j_{t-n_x:t} \in \mathbb{R} \setminus \Omega \\ 0 & \text{otherwise} \end{cases}, \tag{33}$$

and $\mathbb{R} \setminus \Omega = (-\infty, S_x)^{n_x+1}$. As in (28c), the MAR in (32b) is also derived as the average of M indicator functions defined over the set $\mathbb{R} \setminus \Omega$. Now with the FAR and MAR approximations in (28c) and (32b), respectively, the expected-case and worst-case FAR and MAR are obtained by substituting (28c) and (32b) into (13a) – (13b) and (14a) – (14b), respectively.

In summary, given a parameter set $(n_x, S_x) \in \mathbb{N} \times \mathbb{R}$, Algorithm 1 outlines the proposed particle method to approximate the FAR and MAR, as discussed in this section.

Simulation Example

In this section, we consider a on-delay timer alarm design for a non-isothermal continuous stirred tank reactor (CSTR) using the ROC-based method. Assume a CSTR reaction system of volume $\gamma \in \mathbb{R}_+$, and with the following three parallel, irreversible, exothermic reactions

$$\mathrm{A} \xrightarrow{\mathrm{k}_1} \mathrm{B}, \quad \mathrm{A} \xrightarrow{\mathrm{k}_2} \mathrm{U}, \quad \mathrm{A} \xrightarrow{\mathrm{k}_3} \mathrm{R}, \tag{34}$$

where A is the reactant, B is the desired product, and U and R are the undesired byproducts. The concentrations of A, B, U, and R are denoted by C_A, C_B, C_U, and C_R, respectively. The reactor is assembled with a jacket system to remove heat from the reactor. Given (34), the concentrations of species and the reactor temperature are modeled as follows

$$\begin{aligned}\dot{T}(t) =& \frac{1}{\gamma} F(t)(T_{A0} - T(t)) + \sum_{i=1}^{3} \frac{(-\Delta H_i)}{\rho c_p} R_i(C_A(t), T(t)) \\ &+ \frac{Q(t)}{\rho c_p \gamma},\end{aligned} \tag{35a}$$

$$\dot{C}_A(t) = \frac{1}{\gamma} F(t)(C_{A0} - C_A(t)) - \sum_{i=1}^{3} R_i(C_A(t), T(t)), \tag{35b}$$

$$\dot{C}_B(t) = -\gamma^{-1} F(t) C_B(t) + R_1(C_A(t), T(t)), \tag{35c}$$

$$\dot{C}_U(t) = -\gamma^{-1} F(t) C_U(t) + R_2(C_A(t), T(t)), \tag{35d}$$

$$\dot{C}_R(t) = -\gamma^{-1} F(t) C_R(t) + R_3(C_A(t), T(t)), \tag{35e}$$

where: R_i for $i = 1, 2, 3$ are rate functions given by

$$R_i(C_A(t), T(t)) = k_{i0} \cdot exp(-E_i/RT(t))C_A(t); \tag{36}$$

ΔH_i, k_{i0}, and E_i for $i = 1, 2, 3$ denote the enthalpy, pre-exponential rate constant, and the activation energy for the three reactions in (34); T is the reactor temperature; c_p, ρ and R denote the heat capacity, fluid density, and the gas constant, respectively; and Q denote the rate of heat removal. The feed flow rate, denoted by F, is pure A of molar concentration C_{A0} and at temperature T_{A0}. The initial conditions in the CSTR are $T(0) = 300$ K, $C_A(0) = 4$ kmol·m^{-3}, and $C_B(0) = C_U(0) = C_R(0) = 0$ kmol·m^{-3}. Finally, Table 2 gives the nominal values for the parameters used in this simulation.

Discrete-time nonlinear time-series model

The network model in (35) is first discretized and represented in terms of Model 2 using the Euler's discretization method with a time-step 0.01 hr. For the sake of brevity, the discrete time-series model representation of the network in (35) is not shown here, but is straightforward to derive. For the remainder of this section, we assume that the network (35) is represented by Model 2 with $X_t \equiv [T(t)\ C_A(t)\ C_B(t)\ C_U(t)\ C_R(t)]^{\mathrm{T}}$ denoting the process states and $U_t \equiv [F(t)\ Q(t)]^{\mathrm{T}}$ representing the manipulated inputs. To account for discretization error or uncertainties in the parameter values in Table 2, we assume that the state noise in Model 2, denoted by $V_t \sim \mathcal{N}(m_t, Q_t)$ is an additive multivariate Gaussian noise with

$$m_t = \begin{cases} [0\ 0\ 0\ 0\ 0]^{\mathrm{T}} & \text{for } t = 0, \ldots, t_\beta - 1 \\ [0.2\ 0.1\ 0.1\ 0.1\ 0.1]^{\mathrm{T}} & \text{for } t = t_\beta, \ldots, t_N \end{cases}, \tag{37a}$$

$$Q_t = \begin{bmatrix} 0.1 & 0 & 0 & 0 & 0 \\ 0 & 0.1 & 0 & 0 & 0 \\ 0 & 0 & 0.1 & 0 & 0 \\ 0 & 0 & 0 & 0.1 & 0 \\ 0 & 0 & 0 & 0 & 0.1 \end{bmatrix}. \tag{37b}$$

The mean of the state noise in (37a) is assumed to be different in the normal and abnormal operating conditions. It is further assumed that the initial state, $X_0 \in \mathbb{R}^5$ is imprecisely known, such that $X_0 \sim \mathcal{N}(m_{x_0}, Q_{x_0})$, where

$$m_{x_0} = \begin{bmatrix} 300 \\ 4 \\ 0 \\ 0 \\ 0 \end{bmatrix}, \; Q_{x_0} = \begin{bmatrix} 0.01 & 0 & 0 & 0 & 0 \\ 0 & 0.01 & 0 & 0 & 0 \\ 0 & 0 & 0 & 0 & 0 \\ 0 & 0 & 0 & 0 & 0 \\ 0 & 0 & 0 & 0 & 0 \end{bmatrix}. \tag{38}$$

Observe that the initial state distribution is defined independent of the state noise distribution (see Assumption 1). Further, note that even if X_0 and $\{V_t\}_{t\in\mathbb{N}}$ are Gaussian random variables, the distribution for $\{X\}_{t\in\mathbb{N}}$ is non-Gaussian. The non-stationary behavior of $\{X\}_{t\in\mathbb{N}}$ is best elucidated by the reactor temperature profile. Assuming $t_\beta = 75$ hrs and $t_N = 100$ hrs, let Figure 1(a) represent a feed flow rate profile. It is clear from Figure 1(a) that the input signal is proper, as required in Problem 1. For an input profile in Figure 1(a), the reactor temperature profile is given in Figure 1(b). As shown in Figure 1(b), the mean and standard deviation profiles are not only different under the normal and abnormal operations, the profiles are also time-varying within the normal and abnormal operations. This highlights the non-stationary process behavior of of the CSTR reaction system. Note that Figure 1(b) is only shown for illustrative purposes. The ROC-based alarm design for the CSTR reaction system is discussed next.

An ROC-based Alarm Design

In this section, an expected-case and worst-case univariate on-delay timer alarm designs are considered to monitor the concentration of A. Recall that the design parameters for an on-delay timer alarm configuration are the alarm trip point and the delay timer, denoted as $(n_x, S_x) \in \mathbb{N} \times \mathbb{R}$. As discussed earlier, the ROC-based alarm design method chooses an optimal $(n_x, S_x) \in \mathbb{N} \times \mathbb{R}$ by constructing an ROC curve – a trade-off curve between the FAR and MAR for a given $n_x \in \mathbb{N}$ as $S_x \in \mathbb{R}$ is varied. Note that the FAR and MAR for the CSTR reaction network represented by Model 2 are time-varying. For example, Figure 2(a) and (b)

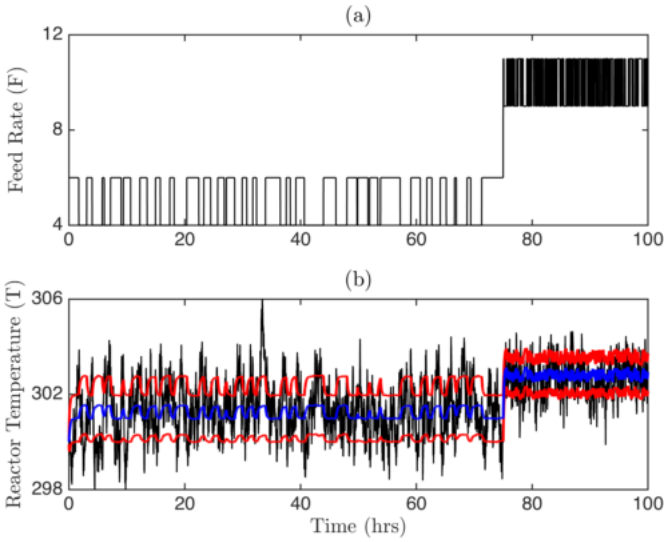

Figure 1: (a) The feed flow rate profile under normal and abnormal operations with fault occurring at $t_\beta = 75$ hrs. The flow rate in the normal and abnormal operations is a random binary signal of specified magnitude and frequency. The change in the flow-rate profile at t_β represent an actuator fault condition. (b) The black curve represents the rector temperature in the normal and abnormal operations. The mean temperature profile is given by the blue curve, and the mean $\pm$ standard deviation profiles are represented in red.

show the FAR and MAR for $n_x = 1$ and $S_x = 5$, respectively, computed using Algorithm 1. From Figure 2(a) and (b) it is clear that the expected-case FAR and MAR (denoted by $F^E(n_x, S_x)$ and $M^E(n_x, S_x)$) are different from their worst-case FAR and MAR (denoted by $F^W(n_x, S_x)$ and $M^W(n_x, S_x)$).

For the ROC-based expected-case alarm design, we construct the ROC curves using $F^E(n_x, S_x)$ and $M^E(n_x, S_x)$. Figure 9 gives the ROC curves for different values of $n_x \in \mathbb{N}$ as $S_x \in \mathbb{R}$ is varied. From Figure 9, it is clear that $F^E(n_x, S_x)$ and $M^E(n_x, S_x)$ decreases as n_x increases. As discussed, seeking an alarm design that yields the smallest $F^E(n_x, S_x)$ and $M^E(n_x, S_x)$ may not be desirable in practice for it also increases the time to detect the fault. Therefore, to ensure practicality of the design, we impose a design requirement which only requires $F^E(n_x, S_x) \leq 7\%$ and $M^E(n_x, S_x) \leq 7\%$.

Table 3 gives a list of alarm trip points for different delay timers and their corresponding $F^E(n_x, S_x)$ and $M^E(n_x, S_x)$ values from the ROC curves in Figure 9. From Table 3 it is clear that the requirements $F^E(n_x, S_x) \leq 7\%$ and $M^E(n_x, S_x) \leq 7\%$ are satisfied for all $n_x \geq 15$. To ensure there is no additional delay

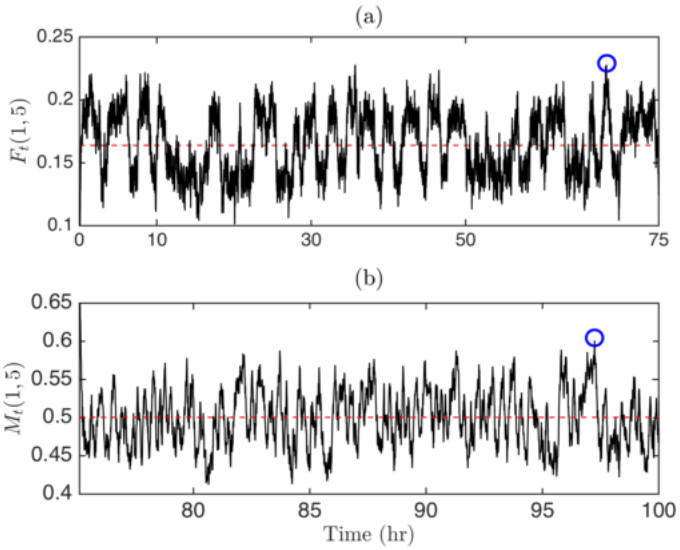

Figure 2: (a) A time-varying profile of $F_t(n_x, S_x)$ is given by the black curve. The average-case FAR, $F^E(n_x, S_x)$ is represented by the broken red curve and the worst-cast FAR, $F^W(n_x, S_x)$ is encircled in blue. (b) (a) A time-varying profile of $M_t(n_x, S_x)$ is given by the black curve. The average-case MAR, $M^E(n_x, S_x)$ is represented by the broken red curve and the worst-cast MAR, $M^W(n_x, S_x)$ is encircled in blue. The profiles are generated using Algorithm 1 for the choice of alarm parameters $n_x = 1$ and $S_x = 5$.

in detecting a fault, we choose the smallest n_x that satisfies $F^E(n_x, S_x) \leq 7\%$ and $M^E(n_x, S_x) \leq 7\%$. From Table 3, the expected-case ROC-based alarm design method selects $(n_x^{R_1} = 15, S_x^{R_1} = 4.73)$ as the optimal choice of the alarm design parameters.

Next we discuss the ROC-based worst-case alarm design procedure to select an optimal $(n_x, S_x) \in \mathbb{N} \times \mathbb{R}$. As previously, Figure 10 give the ROC curves that show the trade-off between $F^W(n_x, S_x)$ and $M^W(n_x, S_x)$ for different values of $n_x \in \mathbb{N}$ as $S_x \in \mathbb{R}$ is varied. As for the expected-case alarm design, observe that $F^W(n_x, S_x)$ and $M^W(n_x, S_x)$ also drop for a higher n_x values; however, notice that the ROC curves in Figure 10 are not as smooth as those in Figure 9. This discrepancy is expected since the worst-case FAR and MAR change considerably for a non-stationary process. Further, observe that for a given $(n_x, S_x) \in \mathbb{N} \times \mathbb{R}$, the worst-case $F^W(n_x, S_x)$ and $M^W(n_x, S_x)$ in Figure 9 are much higher than $F^E(n_x, S_x)$ and $M^E(n_x, S_x)$ in Figure 9.

Finally, Table 4 gives a list of alarm trip points for different delay timers and their corresponding

$F^W(n_x, S_x)$ and $M^W(n_x, S_x)$ values calculated from Figure 10. Now assuming the design constraints $F^W(n_x, S_x) \leq 7\%$ and $M^W(n_x, S_x) \leq 7\%$, from Table 4, the worst-case ROC-based alarm design method selects $(n_x^{R_1} = 25, S_x^{R_2} = 4.72)$ as the optimal choice of the alarm design parameters.

Finally, we perform a Monte-Carlo simulation to check the consistency of the expected-case and worst-case alarm system designs. For the expected-case alarm design, we set $S_x^{R_1} = 4.73$ and $n_x^{R_1} = 15$ samples. We then simulate 5000 new trajectories for C_A by simulating the CSTR reaction system in (35). Figure 11 gives the time-varying FAR and MAR for the simulated trajectories. In Figure 11, the expected FAR and the expected MAR are calculated to be $F^E(n_x^{R_1}, S_x^{R_1}) = 5.61\%$ and $M^E(n_x^{R_1}, S_x^{R_1}) = 5.79\%$, respectively, which are consistent with the values calculated in the design step in Table 3. Similarly, to test the consistency of the worst-case alarm design, we set $S_x^{R_2} = 4.72$ and $n_x^{R_2} = 25$ samples. Using the Monte Carlo samples, the calculated worst-case FAR and MAR are found to be $F^W(n_x^{R_2}, S_x^{R_2}) = 6.46\%$ and $M^W(n_x^{R_2}, S_x^{R_2}) = 6.49\%$, respectively, which are again in agreement with the design values in Table 4.

Conclusions

An efficient alarm system is critical for setting up an efficient fault detection and diagnosis system. While an alarm installation and operations involve a number of key steps, the alarm design has received least attention. This paper considered the problem of industrial alarm design for processes described by stochastic nonlinear time-series models. The proposed alarm design is general and can deal with nonlinear, non-Gaussian, non-stationary, and correlated process dynamics. Mathematical expressions for the false and missed alarm rates – two most common measures of performance for alarm systems – are derived for a delay timer alarm configuration. Due to the lack of a closed-form solution, we use particle methods to compute an approximation of the false and missed alarm rates. Finally, the efficacy of the proposed alarm design was illustrated on a non-stationary reactor system.

Acknowledgment

The first author would like to thank Prof. Swanand R. Khare (Department of Mathematics, Indian Institute of Technology, Kharagpur India) for all the helpful discussions.

References

[1] Tulsyan A, Gopaluni RB. Robust model-based delay timer alarm for non-linear processes. In: *Proceedings of the American Control Conference (ACC)*. Boston, USA. 2016; pp. 2989–2994.

[2] Cochran E, Miller C, Bullemer P. Abnormal situation management in petrochemical plants: can a pilot's associate crack crude? In: *Proceedings of the National Aerospace and Electronics Conference*. Dayton, USA. 1996; pp. 806–813.

[3] Adnan NA, Izadi I, Chen T. On expected detection delays for alarm systems with deadbands and delay-timers. *Journal of Process Control*. 2011;21(9):1318–1331.

[4] Du M, Mhaskar P. Isolation and handling of sensor faults in nonlinear systems. *Automatica*. 2014;50(4):1066–1074.

[5] Du M, Scott J, Mhaskar P. Actuator and sensor fault isolation of nonlinear process systems. *Chemical Engineering Science*. 2013;104:294–303.

[6] Ahnlund J, Bergquist T, Spaanenburg L. Rule-based reduction of alarm signals in industrial control. *Journal of Intelligent and Fuzzy Systems*. 2003;14(9):73–84.

[7] Brooks R, Thorpe R, Wilson J. A new method for defining and managing process alarms and for correcting process operation when an alarm occurs. *Journal of Hazardous Materials*. 2004;115(1):169–174.

[8] Rothenberg D. *Alarm Management for Process Control: A Best-Practice Guide for Design, Implementation, and Use of Industrial Alarm Systems*. Momentum Press. 2009.

[9] Summerhayes C. Deep Water–The Gulf Oil Disaster and the Future of Offshore Drilling. *Underwater Technology*. 2011; 30(2):113–115.

[10] The Buncefield Incident 11 December 2005: The final report of the Major Incident Investigation Board. *Tech. rep.*, Buncefield Major Incident Investigation Board. 2008.

[11] Investigation report: refinery explosion and fire. *Tech. rep.*, US Chemical Safety and Hazard Investigation Board. 2007.

[12] Bingyong Y, Zuohua T, Songjiao S. A novel distributed approach to robust fault detection and identification. *International Journal of Electrical Power and Energy Systems*. 2008;30(5):343–360.

[13] Isermann R. *Fault-diagnosis Systems: an Introduction From Fault Detection to Fault Tolerance*. Springer-Verlag. 2006.

[14] Ding SX. Model-based Fault Diagnosis Techniques: Design Schemes, Algorithms, and Tools.

[15] Engineering Equipment and MAterials Users Association (EEMUA), Alarm Systems- A Guide to Design, Management and Procurement. *EEMUS Publication 191*. 2007;.

[16] International Society of Automation, Management of Alarm Systems for the Process Industries. *ANSI/ISA 182*. 2009;.

[17] EEMUA. *Alarm systems: A guide to design, management and procurement*. EEMUA Publication No. 191 Engineering Equipment and Materials Users Association, London, 2nd ed.

[18] ISA. Management of alarm systems for the process industries. *Tech. rep.*, International Society of Automation. 2009.

[19] Hugo A. Estimation of alarm deadbands. In: *Proceedings of the 7th IFAC Symposium on Fault Detection, Supervision and Safety of Technical Processes*. Barcelona, Spain. 2009; pp. 663–667.

[20] Adnan NA, Cheng Y, Izadi I, Chen T. Study of generalized delay-timers in alarm configuration. *Journal of Process Control*. 2013;23(3):382–395.

[21] Izadi I, Shah S, Kondaveeti S, Chen T. A framework for optimal design of alarm systems. In: *Proceedings of the 7th IFAC Symposium on Fault Detection, Supervision and Safety of Technical Processes*. Barcelona, Spain. 2009; pp. 651–656.

[22] Izadi I, Shah S, David S, Chen T. An introduction to alarm analysis and design. In: *Proceedings of the 7th IFAC Symposium on Fault Detection, Supervision and Safety of Technical Processes*. Barcelona, Spain. 2009; pp. 645–650.

[23] Xu J, Wang J, Izadi I, Chen T. Performance assessment and design for univariate alarm systems based on FAR, MAR, and AAD. *IEEE Transactions on Automation Science and Engineering*. 2012;9(2):296–307.

[24] Kondaveeti SR, Izadi I, Shah SL, Shook DS, Kadali R, Chen T. Quantification of alarm chatter based on run length distributions. *Chemical Engineering Research and Design*. 2013;91(12):2550–2558.

[25] Naghoosi E, Izadi I, Chen T. A study on the relation between alarm deadbands and optimal alarm limits. In: *American Control Conference (ACC), 2011*. San Francisco, USA. 2011; pp. 3627–3632.

[26] Adnan N. Performance Assessment and Systematic Design of Industrial Alarm Systems. Ph.D. thesis, Department of Electrical and Computer Engineering, University of Alberta, Canada. 2013.

[27] Adnan N, Izadi I, Chen T. Computing detection delays in industrial alarm systems. In: *Proceedings of the American Control Conference*. San Francisco, USA. 2011; pp. 786–791.

[28] Tulsyan A, Huang B, Gopaluni RB, Forbes JF. On simultaneous on-line state and parameter estimation in non-linear state-space models. *Journal of Process Control*. 2013;23(4):516–526.

[29] Kondaveeti SR, Izadi I, Shah SL, Chen T. On the use of delay timers and latches for efficient alarm design. In: *Proceedings of the 19th Mediterranean Conference on Control & Automation (MED)*. Corfu, Greece. 2011; pp. 970–975.

[30] Chen J, Gupta AK. *Parametric Statistical Change Point Analysis: with Applications to Genetics, Medicine, and Finance*. Springer Science & Business Media. 2011.

[31] Basseville M, Nikiforov IV. *Detection of Abrupt Changes: Theory and Application*, vol. 104. Prentice Hall Englewood Cliffs. 1993.

[32] Arulampalam MS, Maskell S, Gordon N, Clapp T. A tutorial on particle filters for online nonlinear/non-Gaussian Bayesian tracking. *IEEE Transactions on Signal Processing*. 2002;50(2):174–188.

[33] Tulsyan A, Gopaluni RB, Khare SR. Particle filtering without tears: A primer for beginners. *Computers & Chemical*

Engineering. 2016;95:130–145.

[34] Bullemer P, Nimmo I. A training perspective on abnormal situation management: establishing an enhanced learning environment. In: *Proceedings of the AICHE Conference on Process Plant Safety*. Houston, USA. 1996; .

Algorithm 1 Approximating FAR and MAR

Input: Model 2, a proper input signal $\{U_t\}_{t\in\mathbb{N}}$, time of fault t_β, final time t_N, number of particles M, and alarm parameters (n_x, S_x)

for t=0 to t_N **do**

  if $0 \le t \le n_x - 1$ **then**

    Set $F_t(n_x, S_x) = 0$

  end if

  if $n_x \le t \le t_\beta - 1$ **then**

    Compute an M particle approximation of the joint distribution function $p_N(dx_{t-n_x:t})$ using (27)

$$\tilde{p}_N(dx_{t-n_x:t}) = \frac{1}{M}\sum_{j=1}^{M} \delta_{X^j_{t-n_x:t}}(dx_{t-n_x:t}).$$

    Compute an M particle approximation of FAR using

$$\tilde{F}_t(n_x, S_x) = \frac{1}{M}\sum_{j=1}^{M} \mathbf{1}_\Omega(X^j_{t-n_x:t}),$$

    where $\Omega \triangleq [S_x, +\infty)^{n_x+1}$.

  end if

  if $t_\beta \le t \le t_\beta + n_x - 1$ **then**

    Set $M_t(n_x, S_x) = 1$

  end if

  if $t_\beta + n_x \le t \le t_N$ **then**

    Compute an M particle approximation of the joint distribution function $p_F(dx_{t-n_x:t})$ using (31)

$$\tilde{p}_F(dx_{t-n_x:t}) = \frac{1}{M}\sum_{j=1}^{M} \delta_{\bar{X}^j_{t-n_x:t}}(dx_{t-n_x:t}).$$

    Compute an M particle approximation of MAR using

$$\tilde{M}_t(n_x, S_x) = \frac{1}{M}\sum_{j=1}^{M} \mathbf{1}_{\mathbb{R}\setminus\Omega}(\bar{X}^j_{t-n_x:t}),$$

    where $\mathbb{R} \setminus \Omega = (-\infty, S_x)^{n_x+1}$.

  end if

end for

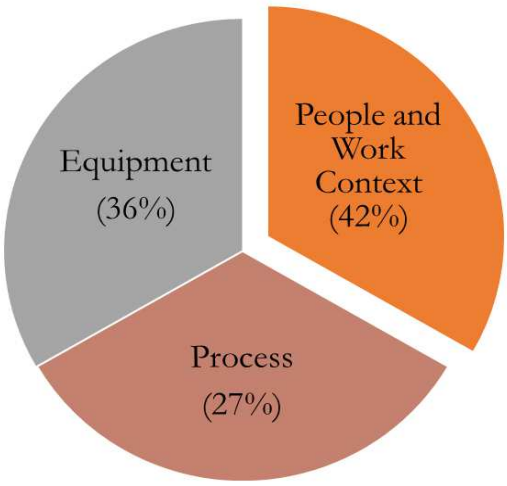

Figure 3: Initiating causes from 1992 plant incident reports. This figure is reproduced from[34] for illustration purposes.

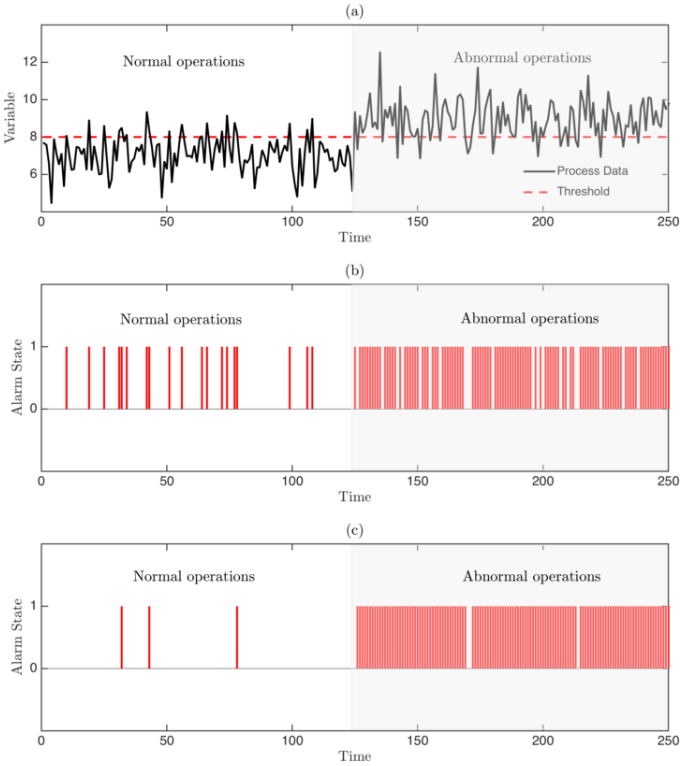

Figure 4: (a) Process data (black-curve) in normal and abnormal operating regions. The normal and abnormal regions are distinguished based on the mean, i.e., the mean value of the variable changes as the process moves from normal to abnormal operating region. The data in the normal region is a Gaussian random variable with mean 7 and variance 1, and the data in the abnormal region is a Gaussian random variable with mean 9 and variance 1. The shaded grey area represents the abnormal operating region. The broken red line represents the alarm threshold. (b) The state of the alarm (represented by the red binary function) in the normal and abnormal regions with zero alarm delay. (c) The state of the alarm (represented by the red binary function) in the normal and abnormal regions with one sample alarm delay. The states 0 and 1 correspond to the alarm "off" and "on" states, respectively.

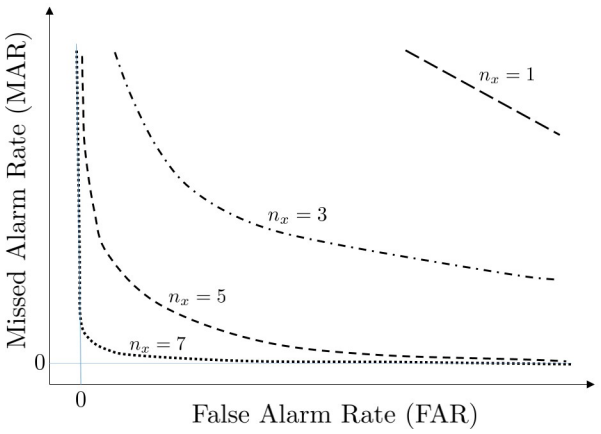

Figure 5: A schematic of ROC curves obtained for an n_x-sample delay timer alarm is shown as S_x is varied in $\mathbb{R}$. The ROC curves corresponding to $n_x = 1, 3, 5$ and 7 are shown here.

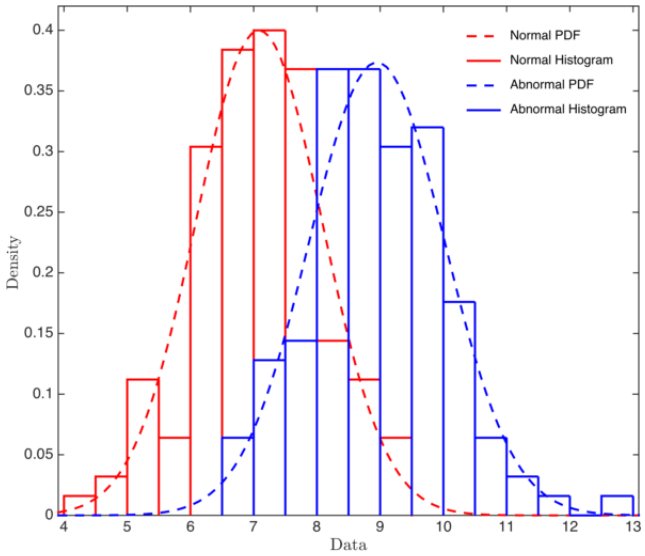

Figure 6: The probability density functions (PDFs) for the variable in Figure 4(a) under normal and abnormal operations. The PDFs in the normal and abnormal regions are represented by the dashed red and blue curves, respectively. The underlying histograms from which these PDFs are estimated are represented by the red and blue staircase functions.

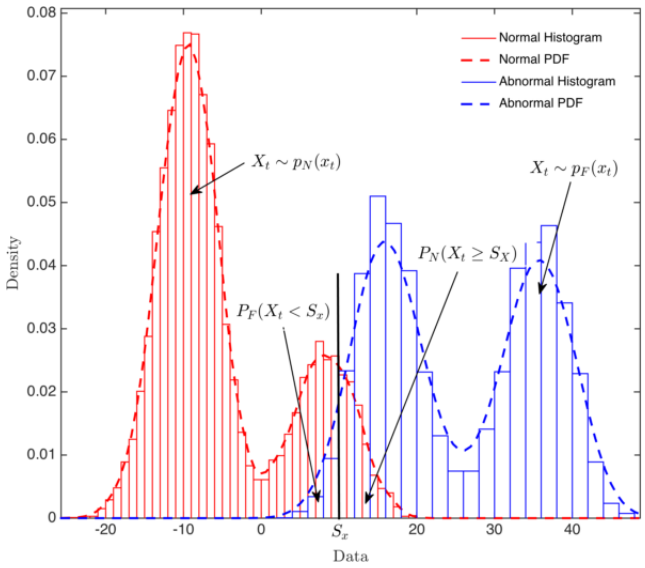

Figure 7: A schematic of the PDFs for $\{X_t\}_{t\in\mathbb{N}}$ in Model 2. The PDF under the normal operation is denoted by $p_N(\cdot)$ (density function in red); and the PDF under the abnormal operations is denoted by $p_F(\cdot)$ (density function in blue). The solid black vertical line denotes the alarm threshold S_x.

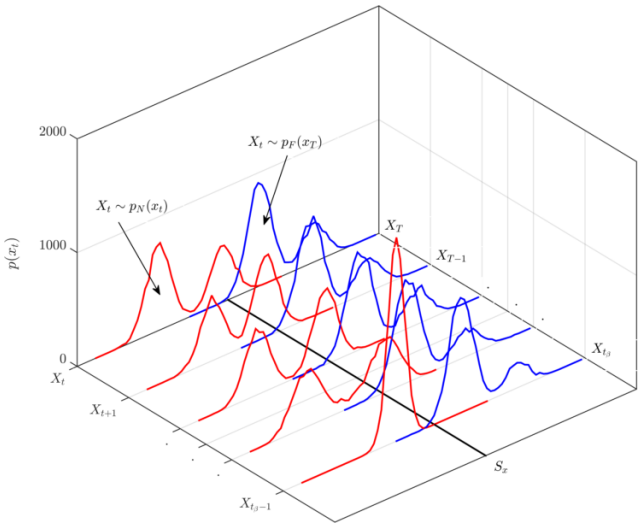

Figure 8: An illustration showing the time-varying density functions for a non-stationary process under normal and abnormal operating conditions. The red density functions correspond to $p_N(\cdot)$ and the blue density functions correspond to $p_F(\cdot)$.

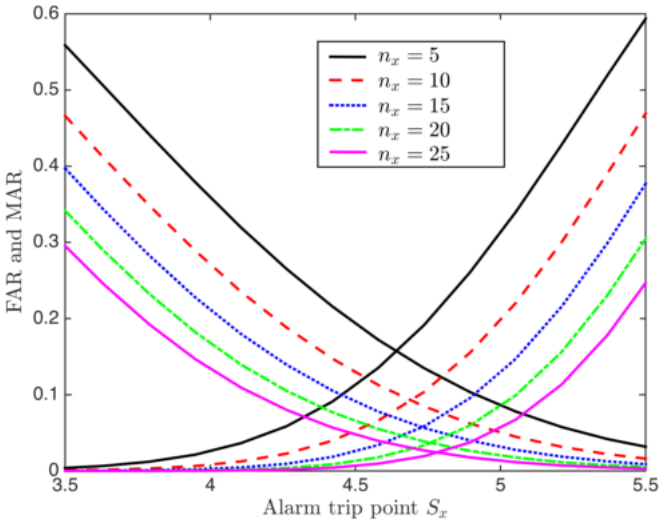

Figure 9: The ROC curves showing the expected-case FAR and MAR calculated for different $(n_x, S_x) \in \mathbb{N} \times \mathbb{R}$ parameter values. The ROC curves are calculated using Algorithm 1 and are shown for $n_x = 5, 10, 15, 20, 25$.

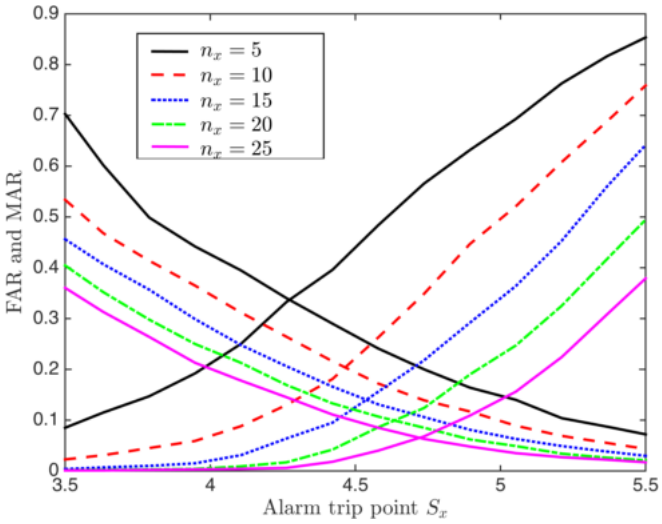

Figure 10: The ROC curves showing the worst-case FAR and MAR calculated for different $(n_x, S_x) \in \mathbb{N} \times \mathbb{R}$ parameter values. The ROC curves are calculated using Algorithm 1 and are shown for $n_x = 5, 10, 15, 20, 25$.

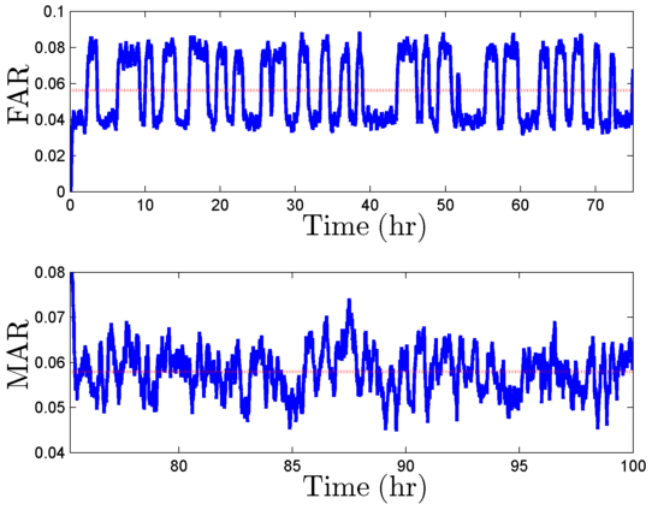

Figure 11: Time-varying FAR and MAR on the cross-validation set generated using Monte-Carlo simulation (denoted here by the blue curves). The expected-case FAR and the expected-case MAR are $F^E(n_x^{R_1}, S_x^{R_1}) = 5.61\%$ and $M^E(n_x^{R_1}, S_x^{R_1}) = 5.79\%$, respectively, where $S_x^{R_1} = 4.73$ and $n_x^{R_1} = 15$ (denoted by broken red lines).

Table 1: (On/Off)-delay time recommendations based on the signal type (EEMUA[17] and ISA[18]).

Signal Type	(On/Off) Delay Timers
Flow rate	15 seconds
Level	60 seconds
Pressure	15 seconds
Temperature	60 seconds

Table 2: Nominal parameter values for the non-isothermal CSTR reaction system considered in (35).

Parameter	**Value**	**Unit**
V	1	m^3
R	8.314	$\mathrm{kJ} \cdot \mathrm{kmol}^{-1} \cdot \mathrm{K}^{-1}$
ΔH_1	-5.0×10^4	$\mathrm{kJ} \cdot \mathrm{kmol}$
ΔH_2	-5.2×10^4	$\mathrm{kJ} \cdot \mathrm{kmol}$
ΔH_3	-5.4×10^4	kJkmol
k_{10}	3.0×10^6	h^{-1}
k_{20}	3.0×10^5	h^{-1}
k_{30}	3.0×10^5	h^{-1}
E_1	5.0×10^4	$\mathrm{kJ} \cdot \mathrm{kmol}^{-1}$
E_2	7.53×10^4	$\mathrm{kJ} \cdot \mathrm{kmol}^{-1}$
E_3	7.53×10^4	$\mathrm{kJ} \cdot \mathrm{kmol}^{-1}$
ρ	1000	$\mathrm{kg} \cdot \mathrm{m}^{-3}$
c_p	0.231	$\mathrm{kJ} \cdot \mathrm{kg}^{-1} \cdot \mathrm{K}^{-1}$

Table 3: Parameter selection chart for the ROC-based expected-case on-delay timer alarm design. The values given here are calculated from Figure 9.

Delay Samples	Alarm Trip (S_x)	FAR=MAR (in %)
5	4.64	15.75
10	4.69	9.28
15	4.73	5.74
20	4.76	3.70
25	4.78	2.43

Table 4: Parameter selection chart for the ROC-based worst-case on-delay timer alarm design. The values given here are calculated from Figure 10.

Delay Samples	Alarm Trip (S_x)	FAR=MAR (in %)
5	4.27	33.69
10	4.45	20.38
15	4.54	14.01
20	4.63	9.93
25	4.72	6.52